Kinetic Evaluation of Substrate-Dependent Origin of the Lag Phase in Soybean Lipoxygenase-1 Catalyzed Reactions†

Zhi-Xin Wang, S. Derek Killilea, and D. K. Srivastava*

Biochemistry Department, North Dakota State University, Fargo, North Dakota 58105

Received August 14, 1992; Revised Manuscript Received October 26, 1992

ABSTRACT: We have measured, under identical conditions, the time courses for the native lipoxygenase (Fe^{2+} form)-catalyzed conversion of linoleic acid into 13-hydroperoxy-9,11-octadecadienoic acid (HPOD) and the oxidation of the Fe^{2+} form of enzyme to the Fe^{3+} form (in 0.1 M borate buffer, pH 10.0, at 25 °C) using a stopped-flow spectrophoto/fluorometer. The experimental results clearly demonstrate that the time course for the appearance of the reaction product is much shorter than that for the conversion of E–Fe^{2+} to E–Fe^{3+}; the latter process involves a pronounced lag phase whereas the former does not. This suggests that the Fe^{2+} form of the enzyme is also catalytically active and that the origin of the lag phase is not intrinsic to the oxidation of the enzyme bound iron cofactor. When the Fe^{3+} form of the enzyme is utilized to investigate the time course of product formation, the lag phase was observed at substrate concentrations higher than 20 μM. The magnitude of this lag phase increases with the increase in the initial concentration of the substrate (at least up to the range where substrate is not dimerized) and decreases in the presence of increasing concentrations of HPOD (exogenously added to the reaction mixture). No lag phase is evident at substrate concentrations in the range of 10 μM or less. We have examined the effects of varied concentrations of substrate and product on the initial rates of the lipoxygenase-catalyzed reaction. In the absence of any externally added HPOD, the initial rate of the enzyme-catalyzed reaction first increases, attains a maximum value, and then starts decreasing at high concentrations of the substrate. Depending upon the range of substrate concentrations, HPOD serves both as an activator (of the inhibited enzymic rate at high substrate concentration) and an inhibitor. At high inhibitory concentrations of the substrate, HPOD (at low concentration) serves as an activator, whereas, at low concentrations of the substrate, HPOD (at high concentration) serves as a competitive inhibitor. A thorough kinetic examination of the lipoxygenase-catalyzed reaction leads us to propose a minimal model according to which (1) the monomeric soybean lipoxygenase-1 possesses at least two classes of binding (viz., catalytic and regulatory) sites, (2) the binding stoichiometry of these two sites are such that the catalytic site can bind either one molecule of substrate or one molecule of product, whereas the regulatory site can bind either two molecules of substrate or one molecule of product, (3) the binding affinities for substrate and product are reciprocally related to their occupancy at catalytic and regulatory sites, respectively, (4) the turnover number of the ES complex is similar to the turnover number of the PES complex (where P is bound at the regulatory site), and (5) the product concentration dependent elimination of the substrate inhibition (reduction of the lag phase) is merely caused by the displacement of substrate from the regulatory site. The steady-state kinetic parameters derived on the basis of this model are adequate to fit the experimentally determined progress curves of the enzyme-catalyzed reaction under diverse experimental conditions.

Soybean lipoxygenase-1 (EC 1.13.11.12) catalyzes the dioxygenation of linoleic acid to form 13-hydroperoxy-9,11-octadecadienoic acid (HPOD) [for reviews, see Vliegenthart and Veldink (1982) and Papatheofanis and Lands (1985)]. The enzyme is a single polypeptide protein of molecular weight 100 000, containing 1 mol of iron cofactor (in its high-spin Fe^{2+} state) per mole of enzyme (Chan, 1973; Roza & Francke, 1973; Pistorius & Axelrod, 1973). During the normal course of catalysis, the Fe^{2+} cofactor is converted into the Fe^{3+} form by the action of the reaction product HPOD, and the latter Fe^{3+} form is maintained during the steady-state turnover of the enzyme (Veldink et al., 1977). The transition in the oxidation state of the iron cofactor is marked by changes in the spectroscopic properties of both the protein and cofactor species. These include (1) the appearance of an EPR signal at $g = 6.1$ due to the transition of the high-spin Fe^{2+} to the high-spin Fe^{3+}, (2) about a 30% decrease in the tryptophan fluorescence, and (3) the appearance of an absorption band at 330 nm (De Groot et al., 1975a,b; Pistorius et al., 1976; Aoshima et al., 1977; Slappendel et al., 1981; Kemal et al., 1987). The enzyme form exhibiting a 330-nm absorption band is known as the "yellow" enzyme, which is converted into a metastable "purple" form (with an absorption maximum at 580 nm) upon interaction with HPOD (De Groot et al., 1975b; Egmond et al., 1977). These, coupled with the intense absorption signal associated with HPOD, have facilitated characterization of this enzyme in considerable detail.

One of the intriguing facets of the lipoxygenase-catalyzed dioxygenation reaction is the existence of a finite induction (lag) period before the onset of the steady-state phase. The magnitude of this "lag" is a function of both the substrate (linoleic acid) and the product (HPOD) concentrations. The lag phase increases at a high concentration of linoleic acid and decreases with an increase in HPOD concentration. Hence, an intricate balance between these variables dictates the nature of the progress curve (the time-dependent appearance of the product) during enzyme turnover. Two models have been proposed to account for the molecular basis of the lag phase,

† Journal article no. 2067 of the North Dakota Agricultural Experiment Station. This work was supported by USDA/CSRS Grants 91-34193-5944 and 90-34216-5417.

* To whom correspondence should be addressed.

0006-2960/93/0432-1500$04.00/0

and its lack thereof, during the lipoxygenase reaction involving diverse conditions of its substrate and the product. These models can be formalistically represented as (1) the product activation model and (2) the substrate inhibition model (Ludwig et al., 1987; Egmond et al., 1976).

According to the first model, the native (Fe^{2+} form) of the enzyme is catalytically inactive. Full catalytic activity of the enzyme is acquired only when the iron cofactor of the enzyme is oxidized from the Fe^{2+} state to the Fe^{3+} state by HPOD. Thus, the origin of the lag phase, according to this model, is intrinsic to the initial slow conversion of the inactive Fe^{2+} form of the enzyme to the fully active Fe^{3+} form by the action of HPOD (either generated as a result of air oxidation of linoleic acid or produced by the contaminant Fe^{3+} form of the enzyme in the native enzyme preparation). Unlike the product activation model, the substrate inhibition model supports the proposition that both Fe^{2+} and Fe^{3+} forms of the enzyme are catalytically active (albeit with different magnitudes); however, they are strongly inhibited at high substrate concentrations due to the binding of the substrate at other (regulatory) sites. The substrate inhibition is envisaged to be slowly overcome as the reaction product (HPOD) accumulates and starts displacing the "inhibitory" substrate from the regulatory site. Thus, according to this model, the origin of the lag phase lies in the differential affinity of the substrate vis a vis the product at the regulatory site of the enzyme. Although both these models have been independently supported by a variety of experimental data, no convincing evidence had yet been presented in favor of one model versus the other.

In pursuit of investigating the mechanistic details of the lipoxygenase-catalyzed reaction, we discovered that the appearance of the initial lag phase is not a consequence of the oxidation of E–Fe^{2+} to E–Fe^{3+}, and it persisted even with the Fe^{3+} form of the enzyme, albeit at high concentrations of linoleic acid (De Groot et al., 1975b). This led us to favor the substrate inhibition model on the first sight. However, the substrate inhibition model, on the basis of this evidence alone, may be criticized since linoleic acid is known to be dimerized at about 60 μM concentration at pH 9.0 (Verhagen et al., 1978a), and the dimeric form of the substrate might be argued to inhibit the enzyme. To avoid kinetic ambiguity arising from the oxidation of E–Fe^{2+} to E–Fe^{3+} during the course of the chemical transformation, we decided to utilize the Fe^{3+} form of the enzyme for all the kinetic experiments. In addition, we selected pH 10.0 to preclude the dimerization of linoleic acid (up to 167 μM) (Verhagen et al., 1978a). As will be shown in the subsequent section, the kinetic analyses at increasing concentrations of linoleic acid have led us to evaluate the binding stoichiometry and affinity for the substrate and the product at different sites on the enzyme molecule.

MATERIALS AND METHODS

Materials. Soybean lipoxygenase (Type I-B) and linoleic acid (highest purity grade, purity higher than 99%) were obtained from Sigma Chemical Co. Other chemicals were of analytical reagent grade. Centricon-30 microconcentrators were purchased from Amicon. The DEAE-FPLC column was a product of EM-separation. Sodium borate buffer (0.1 M, pH 10.0) was used in all experiments unless stated otherwise. All solutions (including buffer) were prepared in Milli-Q purified water.

Methods. Soybean lipoxygenase activity was routinely assayed by monitoring the increase in absorbance at 234 nm due to formation of HPOD (ϵ_{max} = 25 000 M^{-1} cm^{-1}). For determination of specific activities, the enzyme activity was measured in a 0.2 M sodium borate buffer, pH 9.0, containing 23 mg/L Tween 20, utilizing 83 μM linoleic acid as substrate, as described previously by Axelrod et al. (1981). Protein concentration was determined by measuring the absorption at 280 nm ($\epsilon_{280}^{1\%}$ = 14.0; Axelrod et al., 1981).

The commercial preparation of soybean lipoxygenase was further purified by chromatography on a DEAE-FPLC column. The lyophilized enzyme powder was dissolved in a 20 mM sodium phosphate buffer, pH 6.8, and the enzyme solution was loaded onto the DEAE-FPLC column. The adsorbed enzyme was eluted from the column by applying a linear gradient of 20–125 mM sodium phosphate, pH 6.8. The enzyme activity was detected in three peaks. The last peak was judged to be the lipoxygenase-1, from the precedent of its elution profile from an analogous column (Axelrod et al., 1981). The lipoxygenase-1 thus prepared showed a single protein band when subjected to SDS–PAGE analysis. The purified enzyme had a specific activity in the range of 150–180 units/mg under the standard assay conditions (Axelrod et al., 1981).

To avoid oxidation of linoleic acid by atmospheric oxygen, the vial of the highest purity grade linoleic acid (>99% pure) was broken in an anaerobic chamber (flushed with oxygen free argon). The stock aqueous solution of linoleic acid was freshly prepared in 0.1 M borate buffer pH 10.0. At the beginning of each experiment, linoleic acid concentration was enzymatically determined. This (pure) linoleic acid (160 μM) was converted to 13-hydroperoxy-9,11-octadecadienoic acid (HPOD) by incubating with about 0.5 nM purified lipoxygenase-1 in a 0.1 M sodium borate (oxygenated) buffer, pH 10.0, at 4 °C overnight. Under these conditions, 13-HPOD is generated as an exclusive product (Gardner, 1989). The enzyme was removed from the reaction mixture by subjecting it to ultrafiltration through a Centricon-30 microconcentrator. The concentration of HPOD was ascertained by its absorption at 234 nm (ϵ_{234} = 25 000 M^{-1} cm^{-1}).

The Fe^{3+} form of the enzyme was freshly prepared by addition of a 2–3-fold molar excess of linoleic acid to the native enzyme at pH 10.0 and 0 °C and stored at this temperature during the course of the entire experiment. Linoleic acid was quantitatively converted into HPOD with concomitant conversion of the Fe^{2+} form of enzyme to the Fe^{3+} form. The Fe^{3+} enzyme thus prepared either was used as such (in steady-state kinetic experiments) or was separated from the reaction products by repeated centrifugations (at least three times) through the Centricon-30 device (for the HPOD binding experiments). The concentration of HPOD introduced in the enzyme assay system along with the Fe^{3+} form of the enzyme was calculated to be less than 10^{-8} M for all our steady-state kinetic experiments.

The steady-state kinetic experiments were performed at 25 °C (or at 4 °C) on a Lambda 3-B Perkin-Elmer spectrophotometer, interfaced with a personal computer for data acquisition. The reaction mixture (2.5 mL) was continuously stirred by a magnetic stirrer (installed at the bottom of the cuvette holder). This stirring device allowed us to start the reaction and data collection (by computer) within 3 s after initiating the reaction. The rate of conversion of linoleic acid to HPOD was measured at 234 or 250 nm (when the absorption of HPOD was too high). The ϵ for HPOD at 234 nm was judged to be about 3 times higher than that at 250 nm.

Spectrophotometric titration of the Fe^{3+} form of lipoxygenase with HPOD was performed on the same spectrophotometer at 4 °C. A reaction mixture containing 22.3 μM

enzyme in the sodium borate buffer (0.1 M, pH 10.0) was titrated with increasing aliquots of 154.1 μM HPOD in the same buffer, and the increase in absorbance at 580 nm was recorded. The same procedure was repeated by titrating the enzyme, or HPOD solution, separately with increasing aliquots of the buffer. In this way, the decrease in absorption due to dilution of the enzyme was obtained; HPOD does not absorb at 580 nm. The dissociation constant of the enzyme–HPOD complex was determined according to the protocol developed by Wang et al. (1992).

Stopped-flow studies were performed on a DX-17 MV Applied Photophysics spectrophoto/fluorometer system, equipped with a 150-W xenon arc lamp as the light source with full absorption and fluorescence detecting capabilities. The dead time of the instrument was calculated to be 1.34 ms. Four micromolar enzyme (Fe^{2+} form) and 20 μM linoleic acid were mixed at zero time, and the conversion of linoleic acid to HPOD was monitored at 250 nm (since the 234-nm wavelength light was not available due to the presence of the ozone-free xenon light source), and the conversion of E–Fe^{2+} to E–Fe^{3+} was monitored by detecting the fluorescence changes at wavelengths higher than 320 nm following excitation at 280 nm. Instrument control and data collection were performed by an online PC software developed by Applied Photophysics.

Data Analysis. All calculations and simulations were carried out on IBM AT clones with the help of a nonlinear regression analysis program, Enzfitter (Bio-Soft). The initial rates of the enzyme-catalyzed reactions were obtained by fitting the initial parts (from 3 to 20 s) of all the reaction progress curves to second- or third-order polynomial equations in product concentration (Orsi & Tipton, 1979):

$$t = a + b[P] + c[P]^2 + d[P]^3 + \ldots \quad (1)$$

the initial rate, $(d[P]/dt)_{t=0}$, was taken to be a measure of $1/b$ (Philo & Selwyn, 1973).

The dissociation constant for the enzyme–HPOD complex was determined by fitting the experimental results (of Figure 7) by the following equation (Wang et al., 1992):

$$\Delta A = \Delta\epsilon\Big[[P]_0V_0 + [L]_0V_c + K_d(V_0 + V_c) - \sqrt{\{[P]_0V_0 + [L]_0V_c + K_d(V_0 + V_c)\}^2 - 4[P]_0[L]_0V_0V_c}\Big] \Big/ [2(V_0 + V_c)] \quad (2)$$

where $[P]_0$ and V_0 are the initial concentration and volume of the enzyme solution, respectively, and $[L]_0$ is the stock ligand concentration. ΔA and $\Delta\epsilon$ are the absorption changes and the difference in molar extinction coefficient between the complex and the enzyme at 580 nm, respectively. V_c is the total volume of the HPOD solution added during the course of titration.

RESULTS

Catalytic Efficiency of Fe^{2+} versus Fe^{3+} Forms of the Enzyme. To ascertain as to whether the native (Fe^{2+}) form of lipoxygenase must be converted into the Fe^{3+} form before catalyzing the hydroperoxidation of linoleic acid, or if both Fe^{2+} and Fe^{3+} forms of the enzyme are catalytically active, we performed a fast kinetic experiment on a stopped-flow spectrophoto/fluorimetric assembly. The overall strategy was to compare the time-dependent conversion of linoleic acid into HPOD, starting with the Fe^{2+} form of the enzyme, to the conversion of the Fe^{2+} form of the enzyme to the Fe^{3+} form, under identical experimental conditions. If the enzyme activity was given exclusively by the Fe^{3+} form of the enzyme (and the Fe^{2+} form of the enzyme was inactive), the time-dependent conversion of substrate into the product would proceed with a lag phase, due to the slow activation of E–Fe^{2+} to E–Fe^{3+} by HPOD (Ludwig et al., 1987). On the other hand, if both Fe^{2+} and Fe^{3+} forms of the enzyme were catalytically active, no such lag phase would be expected during the progress of the reaction.

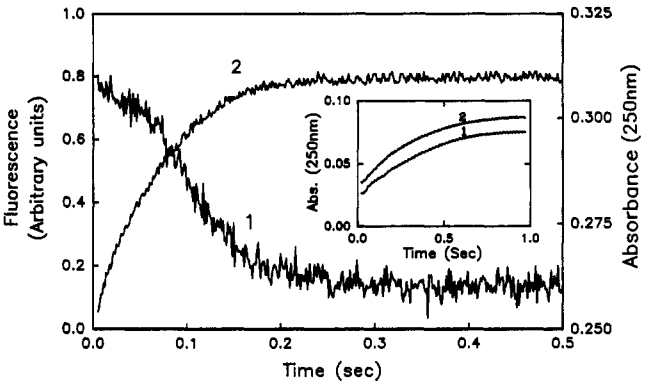

FIGURE 1: Stopped-flow traces for the time-dependent conversion of linoleic acid to HPOD as compared to the oxidation of E–Fe^{2+} to E–Fe^{3+} upon mixing 4 μM native (E–Fe^{2+}) soybean lipoxygenase-1 with 20 μM linoleic acid in a 1:1 ratio (0.1 M sodium borate buffer, pH 10.0, at 25 °C). The E–Fe^{2+} to E–Fe^{3+} conversion was monitored by changes in the protein fluorescence (excitation = 280 nm; emission with a 320-nm cutoff filter) (trace 1). The formation of HPOD was monitored by absorbance changes at 250 nm (trace 2). The inset shows the comparison of the time-dependent increase in absorption at 250 nm upon mixing 17.25 μM linoleic acid with 0.86 μM native enzyme (trace 1), or 0.86 μM Fe^{3+} enzyme plus 3.3 μM HPOD (trace 2) in a 1:1 ratio (in the stopped-flow syringes).

To distinguish between these two alternatives, we measured the time-dependent conversion of linoleic acid to HPOD (by observing the increase in absorbance at 250 nm), and the conversion of E–Fe^{2+} to E–Fe^{3+} (by observing the decrease in protein fluorescence) upon mixing 4 μM (Fe^{2+} form) of lipoxygenase with 20 μM linoleic acid in the stopped-flow syringes at a 1:1 ratio. Figure 1 shows the stopped-flow traces for these two types of reactions. Note that while the decrease in protein fluorescence proceeds with a finite lag phase, no such lag phase is discernible in absorption measurements. Since it is known that the decrease in protein fluorescence is a result of conversion of E–Fe^{2+} to E–Fe^{3+} (Finazzi-Agro et al., 1973, 1975; Kemal et al., 1987), it follows that the latter process is not responsible for the enzyme-catalyzed hydroperoxidation of linoleic acid. When we compared the progress curves of HPOD formation (measured at 250 nm) upon mixing 17.5 μM linoleic acid either with 0.86 μM Fe^{2+} form of the enzyme or with 0.86 μM Fe^{3+} form of the enzyme, we observed remarkable similarity in the progress curves, as well as in the initial rates (inset of Figure 1). These facts lead us to conclude that both these forms of the enzyme are catalytically active. We are currently investigating detailed mechanistic pathways involving both Fe^{2+} and Fe^{3+} forms of the enzyme, and we will report these finding subsequently. A suggestive mechanism as to how Fe^{2+} and Fe^{3+} forms of the enzymes may catalyze hydroperoxidation of linoleic acid has been proposed by Egmond et al. (1977).

Effect of Substrate on Enzyme (Fe^{3+} Form)-Catalyzed Reactions. As reported by others (Kemal et al., 1987; Slappendel et al., 1981), we observed that our freshly prepared (native) enzyme showed a 25–30% quenching of its protein fluorescence upon mixing with HPOD (data not shown). Furthermore, we did not observe any EPR signal representative of Fe^{3+} ion (i.e., signal at $g = 6.1$; Kemel et al., 1987) in our freshly prepared native enzyme (data not shown). These facts

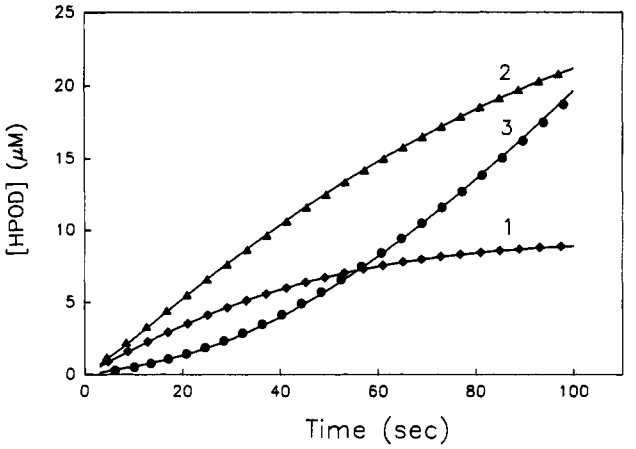

FIGURE 2: Typical examples of the enzyme (Fe^{3+} form)-catalyzed reaction progress curves (monitored at 234 nm) at low, medium, and high concentrations of linoleic acid. The concentrations of linoleic acid for these curves are as follows: (1) 9.76 μM, (2) 27.84 μM, and (3) 139.20 μM. [E-Fe^{3+}] = 2 nM. Other conditions are similar to those of Figure 1. The experimental data are represented by solid lines. The theoretical results (represented by the symbols) were calculated according to eq 17 with kinetic parameters $A_1 = 9.315 \times 10^{-2}\ \mu M^{-1}$, $A_2 = 7.419 \times 10^{-4}\ \mu M^{-2}$, $A_3 = 3.205 \times 10^{-5}\ \mu M^{-3}$, $A_4 = 1.2\ \mu M^{-1}$, and $B_1 = 3.828 \times 10^{-2}\ s^{-1}$.

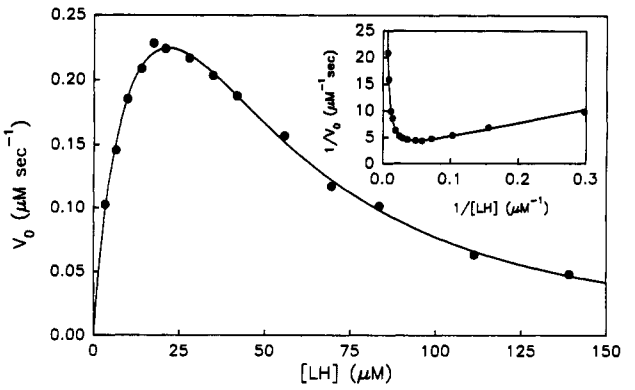

FIGURE 3: Initial rates of the Fe^{3+} form of enzyme-catalyzed formation of HPOD as a function of linoleic acid concentrations. The experimental conditions are same as in Figure 2. The solid line is calculated according to eq 7 with $A_1 = 9.315 \times 10^{-2}\ \mu M^{-1}$, $A_2 = 7.419 \times 10^{-4}\ \mu M^{-2}$, $A_3 = 3.205 \times 10^{-5}\ \mu M^{-3}$ and $B_1 = 3.828 \times 10^{-2}\ s^{-1}$ (see text). The inset shows the double-reciprocal plot of the experimental data.

are suggestive of the iron cofactor of the enzyme being predominantly in the Fe^{2+} form. This, coupled with the fact that the E–Fe^{2+} can catalyze the conversion of linoleic acid to HPOD with an efficiency equal to that of E–Fe^{3+} (inset of Figure 1), led us to ascertain whether the lag phase is observed with the Fe^{3+} form of the enzyme or not, particularly under our experimental conditions (i.e., at linoleic acid concentrations between 3 and 167 μM, pH 10.0, at 25 °C). Thus, we performed all the subsequent experiments using the Fe^{3+} form of the enzyme. Although it is known that, under aerobic conditions, lipoxygenase-1 catalysis yields primarily HPOD as the reaction product (ϵ_{max} = 234 nm), and not side products such as oxodienoic acids, etc. (Kuhn et al., 1986) that absorb at 280 nm, we confirmed this observation under our experimental conditions (data not shown). In this experiment, we could approximate (on the basis that the extinction coefficients of the 234- and 280-nm products are the same; Verhagen et al., 1978b) that no more than 0.6% of the oxo-products would have been formed during the initial period (100 s) of the reaction. Such a low yield of oxo-products eliminates the possibility that the repetitive conversion between stable E–Fe^{2+} and E–Fe^{3+} would have taken place during the catalytic process.

Figure 2 shows the E–Fe^{3+}-catalyzed conversion of linoleic acid to HPOD as a function of time. Note that, at low concentrations of linoleic acid (within a 10 μM concentration range), the time-dependent increase in 234-nm absorption (progress curve) exhibits no lag phase. The lag phase, however, starts appearing as the concentration of linoleic acid is increased, and the reaction progress curves become more sigmoidal in shape. Since the linear parts of the progress curves were too short to be determined accurately by conventional methods (e.g., by drawing a straight line through the experimental points), recourse was made to fit the initial parts (within 20 s) of the reaction progress by the second- or third-order polynomial equation (see Materials and Methods). Figure 3 shows a plot of the substrate concentration-dependent initial rates of the enzyme-catalyzed reaction (obtained by the best fit of the reaction progress curves). Note that as the concentration of linoleic acid increases, the initial rates of the enzyme-catalyzed reaction first increases, attains a maximum value at an intermediary concentration, and then starts decreasing at still higher concentrations of linoleic acid. Such a profile in enzyme kinetics is envisaged to be a result of another substrate binding site on the enzyme molecule (Dixon & Webb, 1979). The rate equation for this two substrate binding site model can be given by

$$v_0 = \frac{B_1[S]}{1 + A_1[S] + A_2[S]^2} \quad (3)$$

Rearrangement of eq 3 yields

$$\frac{1}{v_0} = \frac{1}{B_1}\frac{1}{[S]} + \frac{A_1}{B_1} + \frac{A_2}{B_1}[S] \quad (4)$$

At low substrate concentrations, the third term (i.e., $A_2[S]/B_2$) in eq 4 can be neglected, and the plot of $1/v_0$ against $1/[S]$ should give a straight line with an intercept of A_1/B_1 on the ordinate, and the slope of $1/B_1$. On the other hand, when the substrate concentration is high enough, the first term in eq 4 (i.e., $1/(B_1[S])$) can be neglected, and the plot of $1/v_0$ against [S] should give a straight line with the same intercept of A_1/B_1, but a different slope (A_2/B_1). On the basis of this expectation, when we analyzed the data of Figure 3 according to the two substrate binding site model, we found that although the plot of $1/v_0$ versus $1/[S]$ shows a straight line at low substrate concentrations (inset of Figure 3), and the plot of $1/v_0$ versus [S] is not linear when the substrate concentration is high (Figure 4A). This led us to conclude that the two substrate binding site model (in which the substrate bound at the noncatalytic site inhibits catalysis) is inadequate to explain the experimental results of Figure 3. Assuming that there could be more than two substrate binding sites on the enzyme molecule, we decided to analyze the data of Figure 3 according to a general multisubstrate binding site model as elaborated by Bardsley and Childs (1975):

$$v_0 = \frac{B_1[S] + B_2[S]^2 + B_3[S]^3 + \ldots + B_m[S]^m}{1 + A_1[S] + A_2[S]^2 + A_3[S]^3 + \ldots + A_n[S]^n} \quad (5)$$

where $m < n$. If the enzyme-catalyzed reaction satisfies a fast equilibrium condition, the terms related to $[S]^i$ in eq 5 correspond to the enzyme species that binds with i substrate molecules. The maximum power of the substrate in denominator (n) and numerator (m) of eq 5 corresponds to the total number of substrate binding sites and the total number of noninhibitory sites, respectively. Thus, the difference between n and m (i.e., $r = n - m$) can be taken to be equal to the number of inhibitory sites per enzyme molecule. When any

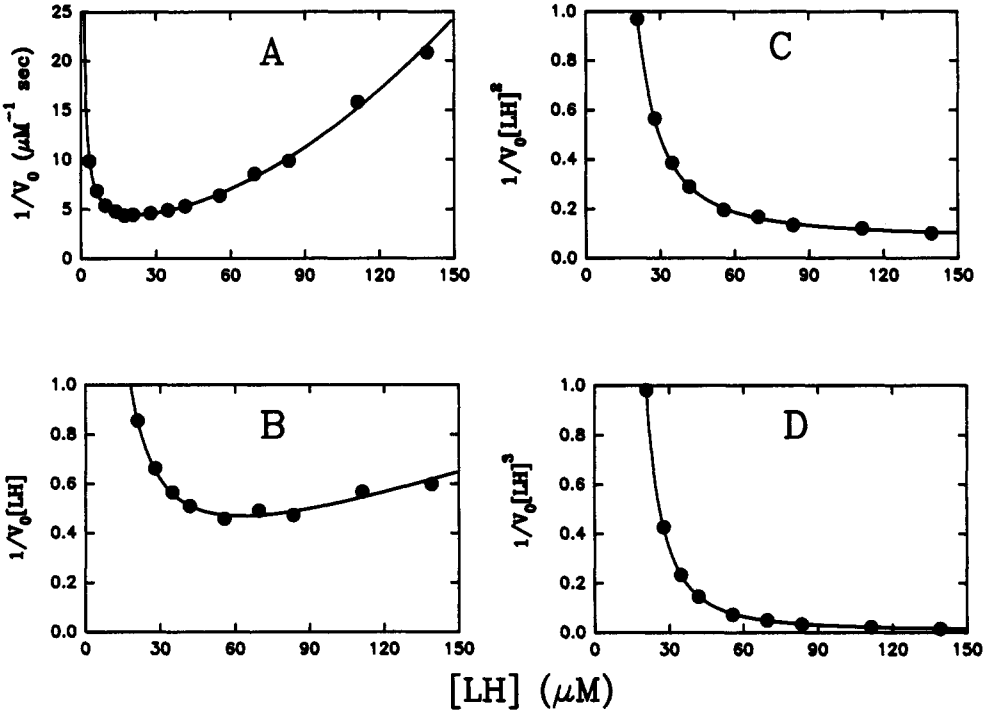

FIGURE 4: Replots of the experimental results of Figure 3 in the form of $1/(v_0[LH]^p)$ versus the concentration of linoleic acid ([LH]) where $p = 0$ (A), $p = 1$ (B), $p = 2$ (C), and $p = 3$ (D). The solid lines represent the calculated lines according to eq 7 with parameters given in Figure 3. The Y-axis values of these comparative plots (B, C, D) are represented in arbitrary units.

one of the r sites is occupied by the substrate, the enzyme is inhibited. Although in principle the value of r can be determined by the graphic methods either of Bardsley and Childs (1975) or of Wang (1990), in practice such analysis is cumbersome due to a nonlinear relationship of these plots. This prompted us to develop an alternate graphical method (a detailed account of which will be published elsewhere) to determine the value of r (i.e., $n - m$). The reciprocal form of eq 5 can be presented as

$$\frac{1}{v_0[S]^p} = \frac{1 + A_1[S] + A_2[S]^2 + A_3[S]^3 + ... + A_n[A]^n}{B_1[S]^{p+1} + B_2[S]^{p+2} + ... + B_m[S]^{p+m}} \quad (6)$$

It can be verified that if one plots $1/(v_0[S]^p)$ against [S] (where $p = 1, 2, 3, ...$) and changes the value of p successively, at sufficiently high concentrations of substrate ([S]), $1/(v[S]^p)$ will have no asymptote if $p < r - 1$; $1/(v_0[S]^p)$ will approach an oblique asymptote if $p = r - 1$; $1/(v_0[S]^p)$ will approach a horizontal asymptote (with the constant term equals to A_n/B_m), if $p = r$; and $1/(v_0[S]^p)$ will approach the abscissa axis if $p > r$. Thus, the number of the inhibition sites in an enzyme molecule ($r = n - m$) can be ascertained by the shapes of $1/(v_0[S]^p)$ versus [S] plots at high substrate concentrations.

Figure 4 shows replots of the experimental data of Figure 3 by varying the p terms as described above. Note that when $p = 2$, the plot exhibits a horizontal asymptote at high substrate concentrations. This suggests that the difference between the maximum power of the denominator to numerator ($n-m$) is 2. A minimal model consistent with this deduction is the one in which the enzyme molecule has a total of three binding sites, out of which only one site is catalytically active and the other two sites are inhibitory. The inhibitory sites can be formalistically assigned as the regulatory sites. The rate equation for such a model can be given by

$$v_0 = \frac{B_1[S]}{1 + A_1[S] + A_2[S]^2 + A_3[S]^3} \quad (7)$$

When the experimental data of Figure 3 were fitted by this equation, a remarkable correspondence was observed. The solid lines in Figures 3 and 4 represent the best fit of the experimental results with parameters $A_1 = 9.315 \times 10^{-2}\ \mu M^{-1}$, $A_2 = 7.419 \times 10^{-4}\ \mu M^{-2}$, $A_3 = 3.205 \times 10^{-5}\ \mu M^{-3}$, and $B_1 = 3.828 \times 10^{-2}\ s^{-1}$.

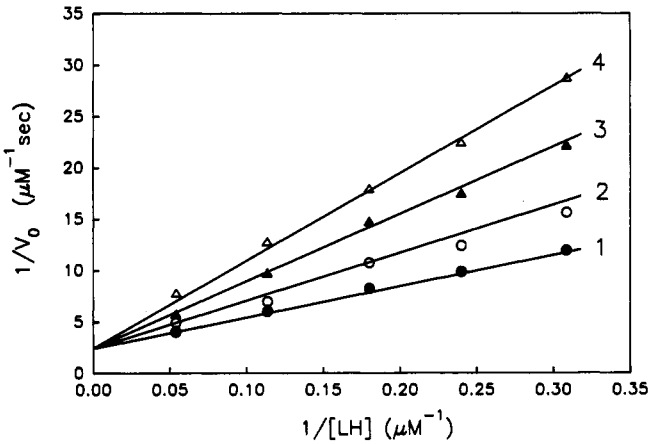

FIGURE 5: Double-reciprocal plot for the rate of HPOD formation as a function of linoleic acid concentration at different (initial) concentrations of HPOD. Due to high initial absorptions of HPOD at 234 nm, the initial rates of HPOD formation were measured at 250 nm spectrophotometrically. [E–Fe^{3+}] = 2 nM. The concentrations of HPOD were 4.61, 38.73, 78.39, and 119.89 μM for curves, 1, 2, 3, and 4, respectively. Other conditions are same as in Figure 2. The solid lines are calculated on the basis of the competitive inhibition model with K_i = 58.92 μM and K_m = 11.63 μM.

Effect of Product on Enzyme (E–Fe^{3+})-Catalyzed Reactions. Having established the two types of substrate binding sites on the enzyme molecule, we became interested in examining the effect of product (HPOD) on enzyme-catalyzed reactions, at both low and high substrate concentrations. We first examined the effects of high concentrations of HPOD on the enzyme-catalyzed reactions involving low concentrations of linoleic acid. Figure 5 shows that product inhibits the enzyme-catalyzed reaction in a competitive manner. The K_i calculated from this plot was found to be 58.92 ± 4.93 μM. It is noteworthy that the K_i for the product is about 5-fold

Table I: Observed Relationships between Kinetic Parameters, Derived from the Best Fit of Progress Curves at Low Substrate Concentrations[a]

initial substrate concentration (μM)	A_4 (μM^{-1})	A_5 (μM^{-2})	B_2 ($\mu M^{-1}.s^{-1}$)	B_2/A_5	A_1A_4
3.36	2.29 ± 0.386	0.227 ± 0.065	0.091 ± 0.015	0.400	0.213
6.44	2.54 ± 0.717	0.171 ± 0.054	0.089 ± 0.026	0.522	0.236
9.76	2.39 ± 0.265	0.195 ± 0.022	0.088 ± 0.010	0.452	0.223

[a] $A_1 = 9.315 \times 10^{-2}\ \mu M^{-1}$ and $B_1 = 3.828 \times 10^{-2}\ s^{-1}$ were used as fixed parameters for fitting the progress curves.

higher than the K_m (11.63 ± 1.16 μM) for the substrate.

It is known that the lag phase in the lipoxygenase-catalyzed reaction (at high substrate concentration) is abolished if the reaction mixture is supplemented with a low concentration of HPOD (Smith & Lands, 1972). This suggested to us that the binding affinity of the product (HPOD) for the regulatory site must be higher than that of the substrate (linoleic acid). At low concentrations of the substrate and the product, the terms of $A_2[S]^2$ and $A_3[S]^3$ in eq 7 can be neglected, and the rate equation in the presence product can be given by

$$\frac{d[P]}{dt} = \frac{B_1[S] + B_2[S][P]}{1 + A_1[S] + A_4[P] + A_5[S][P]} \quad (8)$$

Integration of eq 8 with boundary conditions $t = 0$, $[P] = 0$ gives

$$t = \frac{A_5}{B_2}[P] - \frac{1 + A_4[S]_0}{B_1 + B_2[S]_0}\ln\left(1 - \frac{[P]}{[S]_0}\right) + \left\{\frac{B_2 - B_1A_4}{B_2(B_1 + B_2[S]_0)} + \frac{A_1B_2 - A_5B_1}{B_2^2}\right\}\ln\left(1 + \frac{B_2}{B_1}[P]\right) \quad (9)$$

Given the values of A_1 and B_1 (obtained from the best fit of the experimental data of Figure 3 by eq 7), A_4, A_5, and B_2 can be determined by fitting the progress curves at varied substrate concentrations. Table I shows the fitting results at three low substrate concentrations. It can be seen from Table I that B_2/A_5 is approximately equal to B_1/A_1 and A_5 is approximately equal to the product of A_1 and A_4. This relationship can only be valid if the binding of the product to the regulatory site would exhibit no influence either on the substrate affinity at the catalytic site or on the efficiency of the enzyme-catalyzed reaction (see Discussion).

However, if these relationships (i.e., $B_1/A_1 = B_2/A_5$ and $A_5 = A_1A_4$) are true, then maximum uncertainties lie in the determination of A_4. This can be evident upon simplification of eq 8 as follows:

$$\frac{d[P]}{dt} = \frac{B_1[S] + B_1A_4[S][P]}{1 + A_1[S] + A_4[P] + A_1A_4[S][P]} = \frac{B_1[S]\{1 + A_4[P]\}}{\{1 + A_4[P]\}\{1 + A_1[S]\}} = \frac{B_1[S]}{1 + A_1[S]} \quad (10)$$

Note that eq 10 is in the form of Michaelis–Menten equation. Integration of eq 10 with boundary conditions $t = 0$, $[P] = 0$ yields

$$t = \frac{A_1}{B_1}[P] + \frac{1}{B_1}\ln\frac{[S]_0}{[S]_0 - [P]} \quad (11)$$

We found that eq 11 can fit the progress curves at low substrate concentrations equally well. This finding provided additional support for the relationships $B_2/A_5 = B_1/A_1$ and $A_5 = A_1A_4$. Furthermore, since there is no A_4 term in eq 11, this reemphasized our contention that the magnitude of A_4 could not be determined accurately from the best fit of the progress curves at low substrate concentrations.

In order to determine the value of A_4, we examined the effects of low concentrations of the product on enzyme-catalyzed reactions involving high concentrations of the substrate. At a fixed and high concentrations of the substrate, the initial rate of the enzyme-catalyzed reaction in the presence of a low concentration of the product can be given by

$$v_0 = \frac{1 + C_1[P] + C_2[P]^2 + C_3[P]^3 \ldots + C_m[P]^m}{D_0 + D_1[P] + D_2[P]^2 + D_3[P]^3 + \ldots + D_n[P]^n} \quad (12)$$

where $m \leq n$, and C_i and D_i are the functions of the substrate concentration. These terms are constants at fixed substrate concentrations. When all C_i and D_i terms (where $i > 1$) are equal to zero, eq 12 can be written as

$$v_0 = \frac{1 + C_1[P]}{D_0 + D_1[P]} \quad (13)$$

From eq 13, we have

$$\frac{1}{v_0 - v^*_0} = \frac{D_0^2}{D_0C_1 - D_1}\frac{1}{[P]} + \frac{D_0D_1}{D_0C_1 - D_1} \quad (14)$$

where $v^*_0 = 1/D_0$. As predicted by eq 14, a plot of $1/(v_0 - v^*_0)$ versus $1/[P]$ at a fixed substrate concentration should be a straight line (under conditions where higher order terms of C_i and D_i ($i > 1$) are negligible).

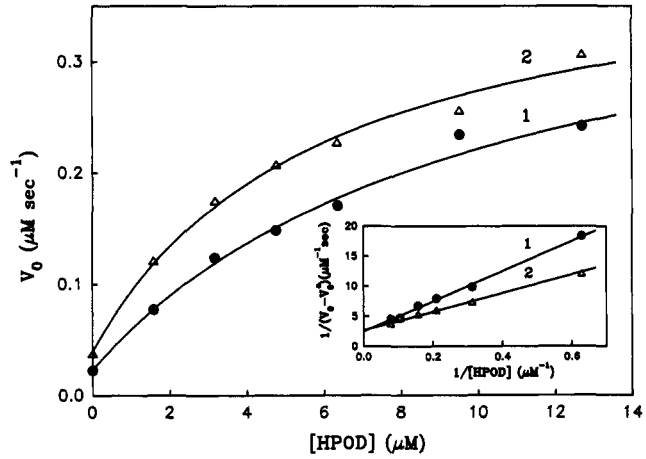

FIGURE 6: HPOD concentration-dependent activation of the enzyme-catalyzed reaction at fixed concentrations of linoleic acid. Linoleic acid concentrations are 160 μM (●) and 118.4 μM (△), respectively. The reaction rates were measured at 234 nm. The inset shows the replots of data as $1/(v_0 - v^*_0)$ vs [HPOD] (where $v_0^* = 1/D_0$). The solid lines are calculated according to eq 13 with parameters $C_1 = 1.84$, $D_0 = 43.6$, and $D_1 = 4.39$ (curve 1) and $C_1 = 1.84$, $D_0 = 25.7$, and $D_1 = 4.54$ (curve 2) (see text). Other conditions are the same as in Figure 2.

Figure 6 shows the effects of the low concentrations of the product on the initial rates of the enzyme-catalyzed reaction at two fixed (and high) concentrations of the substrate. Note a hyperbolic dependence of the initial rates as a function of product concentration. When the data of Figure 6 are reploted as $1/(v_0 - v^*_0)$ versus $1/[P]$, a straight line is observed (see inset, Figure 6). This analysis suggests that the product activation can occur upon binding of one product molecule at the regulatory site of the enzyme. Thus, the overall equation

Table II: Summary of the Observed Kinetic and Thermodynamic Parameters

kinetic/ thermodynamic parameter	value	standard error
A_1	9.315×10^{-2} (μM^{-1})	1.635×10^{-2}
A_2	7.419×10^{-4} (μM^{-2})	3.719×10^{-4}
A_3	3.205×10^{-5} (μM^{-3})	5.873×10^{-6}
A_4	1.841 (μM^{-1})	0.751
B_1	3.828×10^{-2} (s^{-1})	2.62×10^{-3}

to describing our experimental data can be given by

$$\frac{d[P]}{dt} = \frac{B_1[S] + B_2[S][P]}{1 + A_1[S] + A_2[S]^2 + A_3[S]^3 + A_4[P] + A_5[S][P]} \quad (15)$$

If $B_1/A_1 = B_2/A_5$ and $A_5 = A_1A_4$, eq 15 can be rewritten as

$$\frac{d[P]}{dt} = \frac{B_1[S] + B_1A_4[S][P]}{1 + A_1[S] + A_2[S]^2 + A_3[S]^3 + A_4[P] + A_1A_4[S][P]} \quad (16)$$

At a high and fixed concentration of the substrate, the term $A_4[P]$ can be neglected, and a comparison of eqs 16 and 13 shows that $C_1 = A_4$, $D_1 = (A_1A_4)/B_1$, and $D_0 = (1 + A_1[S] + A_2[S]^2 + A_3[S]^3)/(B_1[S])$. According to eq 13, the best fitting results give $C_1 = A_4 = 1.84 \pm 0.751$ μM^{-1} (solid lines in Figure 6). In this way, the accurate value of A_4 could be determined. This determination, in conjunction with others, provides the magnitudes of all the constants of eq 16 (Table II).

We inquired as to whether these constants are adequate to simulate all the progress curves at different substrate concentrations. This test could be performed by simulating these curves by the integrated form of eq 16 with boundary conditions [P] = 0 and t = 0:

$$t = \frac{A_3}{2A_4B_1}[P]^2 + \frac{(A_1A^2_4 - A_2A_4 - A_3 - 2A_3A_4[S]_0)}{B_1A_4^2}[P] - \frac{1}{B_1}\ln\frac{([S]_0 - [P])}{[S]_0} + \frac{A_2A_4(1 + A_4[S]_0) + A_3(1 + A_4[S]_0)^2}{B_1A_4^3}\ln(1 + A_4[P]) \quad (17)$$

In our attempt to simulate the progress curves according to eq 17, we found that all the progress curves can be fitted by using the fixed parameters listed in Table II, except for A_4 = 1.2, and varying the initial concentrations of the substrate by ±5%. For clarity, we show the comparison between calculated results (solid points) vis a vis the experimental data (solid lines) for low, medium, and high substrate concentrations in Figure 2.

Given the kinetic evidence for the existence of two classes of HPOD binding sites, we decided to make an independent measurement of their binding affinities. In this attempt, we realized that although the interaction between the Fe^{3+} form of the enzyme with HPOD can be detected by changes in the spectral properties of the complex, such properties can not be utilized to determine their affinity due to a fairly short lifetime of the complex at 25 °C (Egmond et al., 1977). However, at 4 °C, the intermediary complex has a half-life of 30 min (Egmond et al., 1977). Such a stabilized enzyme–HPOD complex was just adequate to titrate a fixed concentration of enzyme with increasing concentrations of HPOD.

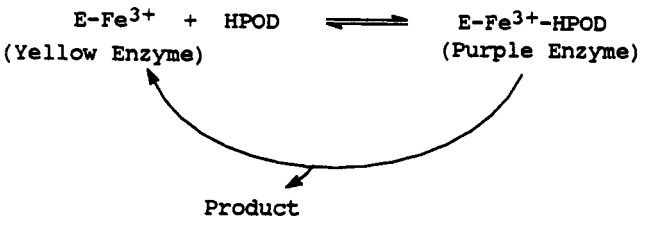

Nevertheless, due to a low extinction coefficient of the enzyme–HPOD complex (1000 M^{-1} cm^{-1}), it was difficult to employ the conventional titration method to determine the dissociation constant of this complex. Recourse was made to the determination of the dissociation constant of the enzyme–HPOD complex by our own developed procedure (Wang et al., 1992), which is especially suitable for conditions where high concentrations of enzymes must be utilized to observe measurable spectroscopic signal changes. Figure 7 shows the increase in absorption at 580 nm upon titration of 22.3 μM enzyme (Fe^{3+} form) with increasing volumes of a fixed concentration of HPOD (157.1 μM). The solid line in Figure 7 is the best fit of the experimental data (see Materials and Methods) for the K_d of the enzyme–HPOD complex to be 41.24 ± 1.22 μM and the difference in molar extinction coefficient between the complex and the free enzyme to be 1189 ± 17 M^{-1} cm^{-1}. The dissociation constant thus determined is similar to the K_i for HPOD (about 60 μM) at 25 °C. To eliminate any ambiguity arising from the temperature effect, we measured the K_i for HPOD at 4 °C and found its value to be about 80 μM (data not shown). This suggests that the K_i values for HPOD at 4 and 25 °C are not much different. Since the dissociation constants of HPOD for the regulatory site versus catalytic sites, obtained from kinetic studies, are about 0.55 and 60 μM, respectively (see Discussion), it is highly plausible that the formation of the purple enzyme from the yellow enzyme is a result of binding of HPOD at the catalytic site.

DISCUSSION

Of the two prevailing models (product activation and substrate inhibition) proposed to account for the existence of the lag phase in the lipoxygenase-catalyzed reaction, the product activation model has received more acceptance in recent years [for reviews, see Vick and Zimmerman (1987)]. This latter model has been supported by the following evidence and arguments: (1) The native enzyme exists in the Fe^{2+} form, which is specifically oxidized by the reaction product HPOD and not by its contemporary analogue, 13(*S*)-hydroxy-9-*cis*,11-*trans*-octadecadienoic acid (HOD); HPOD (but not HOD) is known to eliminate the lag phase in the enzyme-catalyzed reaction involving the native (Fe^{2+}) form of the enzyme (Gibian & Galaway, 1976; Funk et al., 1981). (2) A number of substrate analogues reduce the Fe^{3+} form of enzyme to the Fe^{2+} form and by doing so increase the lag phase of the enzyme-catalyzed reaction (Kemal et al., 1987). (3) A recent kinetic justification that all the reaction progress curves of the lipoxygenase-catalyzed reaction can be adequately described by the product activation model (Ludwig et al., 1987). Among these, the kinetic justification of Ludwig et al. in favor of the product activation model appears to be weak, particularly upon examination of their experimental design. These authors claim that when the Fe^{2+} form of the enzyme is oxidized into the Fe^{3+} form in the presence of HPOD (added in the enzyme reaction mixture), no lag phase is observed at high substrate concentrations, and thus the substrate inhibition model is inappropriate to explain the lag phase (Ludwing et al., 1987). However, in their contention,

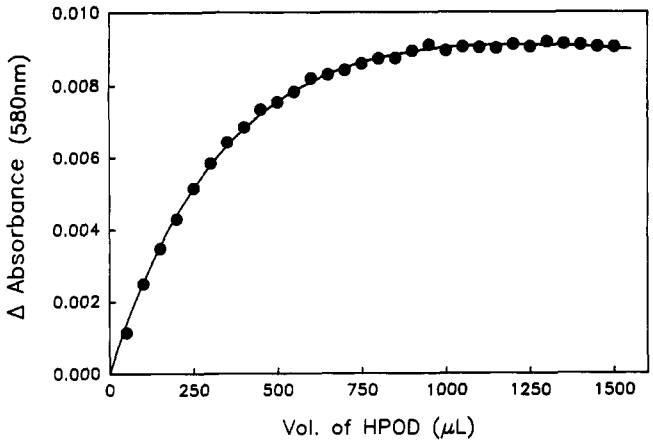

FIGURE 7: Spectrophotometric titration of the ferric form of soybean lipoxygenase-1 with HPOD. A limiting concentration of lipoxygenase (22.3 μM) in a 2.2-mL initial volume (0.1 M sodium borate buffer, pH 10.0) was titrated with increasing aliquots of a stock solution of HPOD (157.1 μM) at 4 °C. The increase in absorbance at 580 nm was recorded after every addition of HPOD. The decrease in absorption of enzyme alone due to the dilution effect has been corrected. The solid line is the best fit of the experimental data according to eq 2 with a dissociation constant of 41.24 μM and $\Delta\epsilon$ of 1189 M^{-1} cm^{-1}.

Ludwig et al. have ignored the influence of free HPOD (i.e., the surplus HPOD after oxidation of E–Fe^{2+} to E–Fe^{3+}) in abolishing the lag phase at high substrate concentrations (see Results). Thus, the experimental results of Ludwig et al. contesting the substrate inhibition model suffer from the lack of appropriate experimental controls.

While this paper was being reviewed for publication, a modified version of the product activation model was published by Schilstra et al. (1992). By incorporating steps involved in the anaerobic cycling of the enzyme under aerobic conditions, Schilstra et al. offered an explanation for the existence of the lag phase in the Fe^{3+} enzyme-catalyzed reaction at high concentration of linoleic acid. However, these authors provided neither any experimental evidence nor any corroborating facts to justify the complexity of their model [see Scheme I of Schilstra et al. (1992)]. In addition, most of the kinetic parameters which are germane to the validity of their model (e.g., k_2, k_3, K_s^*, K_p^*, etc.) were arbitrarily assumed, rather than experimentally determined, particularly for the numerical simulation of their experimental results. Upon cursory examination of their simulation protocol, we have found that the same (assumed) kinetic parameters, which predicted their experimental results at 85 μM linoleic concentration did not satisfactorily predict their experimental results at 26 μM linoleic acid concentration [see Figure 1 of Schilstra et al. (1992)]. In addition, these authors assumed the value of k_2 to be 1.5×10^6 s^{-1}, which is too fast to satisfy the rapid equilibrium conditions, and thus their overall theoretical treatment is questionable. Furthermore, the inability of HOD (rather than HPOD) to abolish the lag phase (evidence in favor of the product activation model) could simply be a result of impaired binding of HOD at the regulatory site of the enzyme. Thus, despite a widespread belief in favor of the product activation model, no unequivocal experimental evidence has yet been presented to substantiate it.

Toward this end, we decided to elucidate the mechanistic origin of the lag phase in the lipoxygenase-catalyzed reaction, particularly at high substrate concentrations. In this pursuit, we performed most of the experiments utilizing Fe^{3+} form of the enzyme with due care: (1) to minimize the transfer of free HPOD along with the enzyme (the Fe^{3+} form of the enzyme is prepared by addition of a slight molar excess of linoleic acid to the native enzyme) in the reaction mixture and (2) to limit the variability of the substrate concentration, such that the dimeric form of the linoleic acid could be precluded. The first objective was achieved by incubating about 1 μM native enzyme with 2–3 μM linoleic acid to yield a stock Fe^{3+} enzyme mixture at 0 °C, and since each time 5 μL of this mixture was utilized to start the reaction (total volume – 2.5 mL), less than 10 nM HPOD was transferred to the reaction mixture along with the enzyme. Such a small concentration of HPOD can be argued to have no effect for eliminating the lag phase, particularly since its binding constant at the regulatory site is about 0.55 μM. In addition, no effect of HPOD on the reaction progress curve was discerned when the stock Fe^{3+} enzyme preparation was allowed to age for about 8 h at 0 °C. The second objective was naturally met, when we performed all our experiments at pH 10.0 and limited the variation of substrate concentrations up to 167 μM; under this condition linoleic acid dimerization is known not to occur (Verhagen et al., 1978a). Given these restrictive conditions, it is unlikely that our experimental results can in any way be explained by the product activation model. Instead, all the experimental results, as well as the detailed kinetic analysis, support the substrate inhibition model.

Scheme I

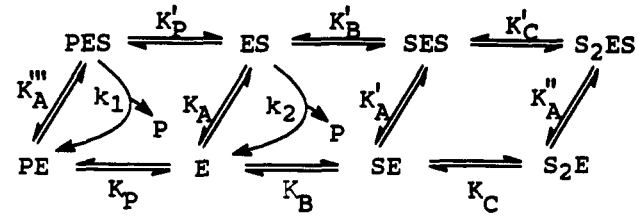

Our kinetic analyses for the substrate concentration-dependent lipoxygenase-catalyzed reaction rates reveal that although there is one catalytic site within the enzyme molecule, there are two regulatory sites. It must be pointed out that our kinetic method cannot distinguish between the two physically distinct sites versus only one physical site where two substrate molecules can bind and inhibit the reaction. Since the inhibitory influence of the substrate is overcome upon binding of only one product molecule, it is plausible that the two substrate molecules bind at a common physical site in the form of a substrate dimer, and they are competitively displaced by one molecule of the product. Such a possibility can be supported by the precedents that linoleic acid tends to form a dimer at high concentrations (Verhagen et al., 1978a). However, irrespective of the molecular complexity of the enzyme, the kinetic results are consistent with the model of Scheme I.

In Scheme I, E, S, and P refer to the enzyme, substrate, and product, respectively. S or P on the left hand side of E denotes the binding of these species on the regulatory site of the enzyme, whereas S on right side denotes its binding on the active site. Due to the weak affinity of the product to the catalytic site, the species involving P at the catalytic site are not considered in Scheme I. To simplify kinetic results, all the association/dissociation steps involving substrate and product are assumed to be in rapid equilibrium. K_A, K_B, etc. represent the dissociation constants of appropriate complexes, whereas k_1, k_2, etc. represent the rate constants. This kinetic scheme is adequately described by eq 15, derived from the analysis of experimental data. The macroscopic terms of this equation exhibit the following relationships with the microscopic constants of Scheme I (see Appendix):

$$A_1 = \frac{1}{K_A} + \frac{1}{K_B}$$

$$A_2 = \frac{1}{K_A K'_B} + \frac{1}{K_B K_C}$$

$$A_3 = \frac{1}{K_A K'_B K'_C}$$

$$A_4 = \frac{1}{K_p}$$

$$A_5 = \frac{1}{K_A K'_p}$$

$$B_1 = \frac{k_1[E]_0}{K_A}$$

$$B_2 = \frac{k_2[E]_0}{K_A K'_p}$$

Before deriving conclusions from the measured macroscopic parameters and their relationships to the microscopic constants of Scheme I, we do note that the affinity of HPOD for the catalytic site (K_i = 60 μM) is about 5 times weaker than the affinity for linoleic acid (K_m = 11 μM) for the same site. At this point, it should be pointed out that the dissociation constant for the E–Fe^{3+}–HPOD complex at 4 °C (41 μM) is remarkably similar to the K_i for the HPOD at 25 °C (or 4 °C). Thus, in contrast to previous conclusions, we believe that HPOD binds at the catalytic site of the yellow (Fe^{3+} form) enzyme, and, consequent upon this binding, the yellow enzyme is converted into the purple enzyme. This belief is strengthened by the fact that the purple enzyme slowly turns over to yield a hydroxy fatty acid as a reaction product (Garssen et al., 1972; Egmond et al., 1977), and such an event is unlikely to occur at a site other than the catalytic site.

Unlike the inhibitory effect of high levels of HPOD in the lipoxygenase-catalyzed reaction at low substrate concentrations, low levels of HPOD activate the enzyme-catalyzed reaction when the substrate concentration is high, i.e., in the inhibitory range. From the HPOD concentration-dependent activation data of Figure 6, we calculated the value of A_4 to be 1.84 μM^{-1}. This value is translated into the dissociation constant of HPOD from the regulatory site (0.55 μM) of the enzyme by the relationship $A_4 = 1/K_p$. This suggests that the affinity of HPOD for the regulatory site is at least two orders of magnitude higher than that for the catalytic site. On the other hand, when we compare the affinity of the substrate for the catalytic site vis a vis its affinity for the first substrate binding at the regulatory site (the apparent affinity of the latter can be taken to be the ratio of A_2 to A_1), the opposite relationship is discerned. Hence, the affinity of the substrate at the catalytic site is at least an order of magnitude higher than that at the regulatory site. Given this comparison, it is reasonable to accept that A_1 is a measure of $1/K_A$. This differential affinity of the product versus the substrate provides a molecular explanation for the origin of the lag phase at high substrate concentrations.

As elaborated under Results, the data of Table I provide two independent correlations, viz., $B_1/A_1 = B_2/A_5$ and $A_5 = A_1A_4$. When these relationships were analyzed in the light of the microscopic parameters of Scheme I, few important conclusions were discerned. Given that the A_1 is measure of $1/K_A$, $B_1/A_1 = k_1[E]_0$ and $B_2/A_5 = k_2[E]_0$. If $B_1/A_1 = B_2/A_5$, it must imply that $k_1 = k_2$. This means that the turnover of the ES complex is equal to the turnover of the PES complex. In other words, the binding of the product at the regulatory site does not influence the catalytic turnover of the substrate. Similarly, the relationship $A_5 = A_1A_4$ can be shown to be valid only under condition where $K_p = K_p'$. This implies that the binding of the product at the regulatory site is not affected by the prior occupancy of the substrate at the catalytic site. These generalizations lead us to conclude that, despite the existence of two types of binding sites in the lipoxygenase molecule, enzyme catalysis is affected only by the presence of substrate (and not by the presence of product) at the regulatory site. Thus, the product activates substrate-inhibited enzyme activity by merely displacing the substrate from the regulatory site.

APPENDIX

For kinetic model of Scheme I, the dissociation constants for various enzyme substrate/product species can be given by following equations:

$$\frac{[E][S]}{[ES]} = K_A \qquad \frac{[E][S]}{[SE]} = K_B \qquad \frac{[ES][S]}{[SES]} = K_B'$$

$$\frac{[SE][S]}{[S_2E]} = K_C \qquad \frac{[SES][S]}{[S_2ES]} = K_C' \qquad \frac{[E][P]}{[PE]} = K_p$$

$$\frac{[ES][P]}{[PES]} = K_p'$$

These equations can be arranged to yield

$$[ES] = [E][S]/K_A \qquad [SE] = [E][S]/K_B$$

$$[SES] = [E][S]^2/K_AK_B' \qquad [S_2E] = [E][S]^2/K_BK_C$$

$$[S_2ES] = [E][S]^3/K_AK'_BK'_C \qquad [PE] = [E][P]/K_p$$

$$[PES] = [E][S][P]/K_AK_p'$$

Since the total concentration of the enzyme ($[E]_0$) is fixed, its distribution in different forms of enzyme–substrate/product complexes can be given by

$$[E]_0 = [E] + [ES] + [SE] + [SES] + [S_2E] + [S_2ES] + [PE] + [PES]$$

Upon substituting the values for different enzyme–substrate species, we obtain

$$[E]_0 = [E]\left\{1 + \left(\frac{1}{K_A} + \frac{1}{K_B}\right)[S] + \left(\frac{1}{K_AK_B'} + \frac{1}{K_BK_C}\right)[S]^2 + \frac{1}{K_AK_B'K_C'}[S]^3 + \frac{1}{K_p}[P] + \frac{1}{K_AK_p'}[P][S]\right\} = [E]R$$

where R represents the combined terms contained in the parentheses. The enzyme species [E], [ES], and [PES] are related to R by the following equations:

$$[E] = \frac{[E]_0}{R} \qquad [ES] = \frac{[S][E]_0/K_A}{R}$$

$$[PES] = \frac{[S][P][E]_0/K_AK_p'}{R}$$

Since both [ES] and [PES] are the productive enzyme–substrate complex species, the overall rate equation for the enzyme catalyzed reaction can be given by

$$v = k_1[ES] + k_2[PES] = \frac{k_1[S][E]_0/K_A + k_2[S][P][E]_0/K_AK_p'}{R}$$

This equation can be rearranged to obtain eq 15 (see the text). The quantitative relationships between macroscopic and the microscopic parameters can thus be given by the equations given under Discussion.

REFERENCES

Aoshima, H., Kajiwara, T., Hatanaka, A., Nakatani, H., & Hiromi, K. (1977) *Biochim. Biophys. Acta 486*, 121–126.

Axelrod, B., Cheesbrough, T. M., & Laakso, S. (1981) *Methods Enzymol. 71*, 441–451.

Bardsley, W. G., & Childs, R. E. (1975) *Biochem. J. 149*, 313–328.

Chan, H. W.-S. (1973) *Biochim. Biophys. Acta 327*, 32–35.

Clapp, C. H., Banerjee, A., & Rotenberg, S. A. (1985) *Biochemistry 24*, 1826–1830.

De Groot, J. J. M. C., Veldink, G. A., Vliegenthart, J. F. G., Boldingh, J., Wever, R., & van Gelder, B. F. (1975a) *Biochim. Biophys. Acta 377*, 71–79.

De Groot, J. J. M. C., Garssen, G. J., Veldink, G. A., Vliegenthart, J. F. G., Boldingh, J., & Egmond, M. R. (1975b) *FEBS Lett. 56*, 50–54.

Dixon, M., & Webb, E. C. (1979) *Enzymes*, 3rd ed., Academic Press, New York.

Egmond, M. R., Finazzi Agro, A., Fasella, P. M., Veldink, G. A., & Vliegenthart, J. F. G. (1975) *Biochim. Biophys. Acta 397*, 43–49.

Egmond, M. R., Brunori, M., & Fasella, P. M. (1976) *Eur. J. Biochem. 61*, 93–100.

Egmond, M. R., Fasella, P. M., Veldink, G. A., Vliegenthart, J. F. G., & Boldingh, J. (1977) *Eur. J. Biochem. 76*, 469–479.

Finazzi-Agro, A., Avigliano, L., Veldingk, J., Vliegenthart, J. F. G., & Boldingh, J. (1973) *Biochim. Biophys. Acta 326*, 462–470.

Finazzi-Agro, A., Avigliano, L., Egmond, M. R., Veldink, G. A., & Vliegenthart, J. F. G. (1975) *FEBS Lett. 52*, 73–76.

Funk, M. O., Kim, S. H.-S., & Alteneder, A. W. (1981) *Biochem. Biophys. Res. Commun. 98*, 922–929.

Gardner, H. W. (1989) *Biochim. Biophys. Acta 1001*, 274–281.

Garssen, G. J., Vliegenthart, J. F. G., & Boldingh, J. (1971) *Biochem. J. 122*, 327–332.

Garssen, G. J., Vliegenthart, J. F. G., & Boldingh, J. (1972) *Biochem. J. 130*, 435–442.

Gibian, M. J., & Galaway, R. A. (1976) *Biochemistry 15*, 4209–4214.

Hainig, J. L., & Axelrod, B. (1958) *J. Biol. Chem. 232*, 193–202.

Kemal, C., Louis-Flamberg, P., Krupinski-Olsen, R., & Shorter, A. L. (1987) *Biochemistry 26*, 7064–7072.

Kuhn, H., Salzmann-Reinhardt, U., Ludwig, P., Ponicke, K., Schewe, T., & Rapoport, S. (1986) *Biochim. Biophys. Acta 900*, 187–193.

Ludwig, P., Holzhutter, H., Colosimo, A., Silvestrini, M. C., Schewe, T., & Papoport, S. M. (1987) *Eur. J. Biochem. 168*, 325–337.

Orsi, B. A., & Tipton, K. F. (1979) *Methods Enzymol. 63*, 159–183.

Papatheofanis, F. J., & Lands, W. E. M. (1985) in *Biochemistry of Arachidonic Acid Metabolism* (Lands, W. E. M., Ed.) pp 9–39, Mentinus Nijloff, Boston.

Philo, R. D., & Selwyn, M. J. (1973) *Biochem. J. 135*, 525–530.

Pistorius, E. K., & Axelrod, B. (1973) *Fed. Proc. 32*, 554.

Pistorius, E. K., Axelrod, B., & Palmer, G. (1976) *J. Biol. Chem. 251*, 7144–7148.

Roza, M., & Francke, A. (1973) *Biochim. Biophys. Acta 327*, 24–31.

Schilstra, M. J., Veldink, G. A., Verhagen, J., & Vliegenthart, J. F. G. (1992) *Biochemistry 31*, 7692–7699.

Slappendel, S., Veldink, G. A., Vliegenthart, J. F. G., Aasa, R., & Malmstrom, B. G. (1981) *Biochim. Biophys. Acta 667*, 77–86.

Smith, W. L., & Lands, W. E. M. (1972) *J. Biol. Chem. 247*, 1038–1047.

Veldink, G. A., Vliegenthart, J. F. G., & Boldingh, J. (1977) *Prog. Chem. Fats Other Lipids 15*, 131–166.

Verhagen, J., Vliegenthart, J. F. G., & Boldingh, J. (1978a) *Chem. Phys. Lipids 22*, 255–259.

Verhagen, J., Veldink, G. A., Egmond, M. R., Vliegenthart, J. F. G., Boldingh, J., & Star, J. V. D. (1978b) *Biochim. Biophys. Acta 529*, 369–379.

Vick, B. A., & Zimmerman, D. C. (1987) in *The Biochemistry of Plants* (A Comprehensive Treatise) (Stumf, P. K., & Conn, E. E., Eds.) Vol. 9, pp 53–89, Academic Press, New York.

Vliegenthart, J. F. G., & Veldink, G. A. (1982) in *Free Radicals in Biology* (Pryor, W. A., Ed.) Vol. 5, pp 29–64, Academic Press, New York.

Wang, Z. X. (1990) *J. Theor. Biol. 143*, 465–472.

Wang, Z. X., Kumar, R., & Srivastava, D. K. (1992) *Anal. Biochem.* (in press).